

# MC<sup>2</sup>: Multi-concept Guidance for Customized Multi-concept Generation

Jiaxiu Jiang, Yabo Zhang, Kailai Feng, Xiaohe Wu, and Wangmeng Zuo<sup>✉</sup>

Harbin Institute of Technology

**Abstract.** Customized text-to-image generation aims to synthesize instantiations of user-specified concepts and has achieved unprecedented progress in handling individual concept. However, when extending to multiple customized concepts, existing methods exhibit limitations in terms of flexibility and fidelity, only accommodating the combination of limited types of models and potentially resulting in a mix of characteristics from different concepts. In this paper, we introduce the **Multi-Concept** guidance for **Multi-Concept** customization, termed **MC<sup>2</sup>**, for improved flexibility and fidelity. MC<sup>2</sup> decouples the requirements for model architecture via inference time optimization, allowing the integration of various heterogeneous single-concept customized models. It adaptively refines the attention weights between visual and textual tokens, directing image regions to focus on their associated words while diminishing the impact of irrelevant ones. Extensive experiments demonstrate that MC<sup>2</sup> even surpasses previous methods that require additional training in terms of consistency with input prompt and reference images. Moreover, MC<sup>2</sup> can be extended to elevate the compositional capabilities of text-to-image generation, yielding appealing results. Code will be publicly available at <https://github.com/JIANGJiaXiu/MC-2>.

**Keywords:** Text-to-image generation · Customized multi-concept generation · Compositional generation

## 1 Introduction

Diffusion models have facilitated advancements in creative visual generation [18, 36, 40, 42, 45, 54]. Leveraging the power of text-to-image diffusion models, customized generation [13, 15, 16, 25, 32, 38, 43, 47, 49, 50, 53] enables users to craft images aligned with their personalized concepts. While earlier endeavors [13, 43, 49] predominantly address the intricacies of single-concept customization, the challenge persists when it comes to multi-concept customization in terms of flexibility and fidelity.

Existing works performs customized multi-concept generation through joint training [16, 25] or merging single-concept customized models [15, 29, 38, 47]. Joint training [16, 25] requires access to the reference images of the specified concepts, and retrain all parameters when introducing a new concept. Merging single-concept customized models [15, 29, 38, 47] promisingly reduces the training cost.

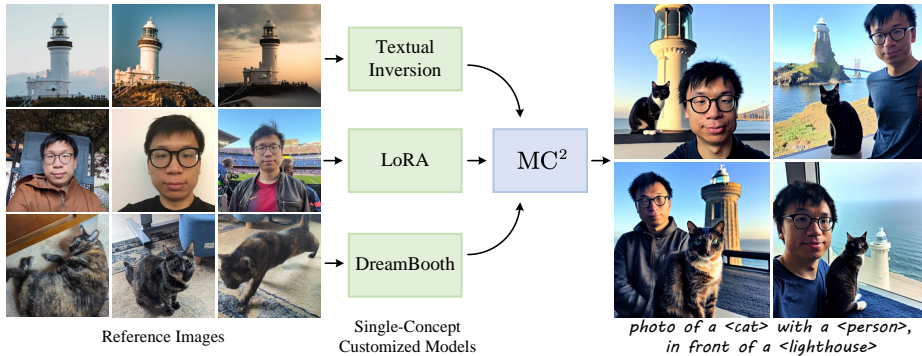


**Fig. 1: Overview of our method.** MC<sup>2</sup> composes separately trained customized models to generate compositions of multiple customized concepts. Here, we train a Textual Inversion [13] model for <lighthouse>, a LoRA [21] for <person>, and a DreamBooth [43] model for <cat> with the reference images of each concept. The reference images are from the CustomConcept101 dataset [25].

Nonetheless, it is challenging for the above methods to integrate multiple heterogeneous single-concept customized models, as they require specific network architectures and access to training data. Users may obtain a large amount of single-concept customized models from the community, but cannot acquire their training data in most cases. Therefore, these models are difficult to be integrated to generate compositions of multiple customized concepts. Albeit Cones-2 [30] does not require joint training or model merging for generating composition of customized concepts, it introduces additional and inconvenient condition signals, *e.g.*, bounding boxes or segmentation masks. Encoder-based customization methods [32, 50] usually involve finetuning the pretrained text-to-image diffusion model to accept identity information extracted from the reference images, which are orthogonal to our work.

To address the above mentioned problems, we propose the **Multi-Concept** guidance for customized **Multi-Concept** generation, termed **MC<sup>2</sup>**. Our proposed MC<sup>2</sup> facilitates the seamless integration of separately trained heterogeneous single-concept customized models, allowing for the natural synthesis of a composition of their distinct concepts without additional training. As shown in Fig. 1, a Textual Inversion [13] model, a LoRA [21] and a DreamBooth [43] model are combined with our method, demonstrating its versatility without requiring extra training or additional conditioning information. Multi-concept guidance (MCG) acts as an avenue for the separately trained customized models to communicate with each other. In each step of MC<sup>2</sup>, each customized model denoises the same latent noise map respectively, then MCG attempts to identify the activated regions of each concept and spatially disentangle them. When the activated regions of each concept have little overlap, the multiple customized concepts are more likely to be generated simultaneously with less incorrect attribute binding. Inspired by [7, 35, 46], we extract the cross-attention maps from the diffusion

process. Certain cross-attention maps indicate the activated regions of each customized concept. Then MCG adaptively refines the attention weights between visual and textual tokens, directing image regions to focus on their associated words while diminishing the impact of irrelevant ones. Moreover, MC<sup>2</sup> can be extended to enhance the compositional generation ability of existing text-to-image diffusion models, yielding appealing results.

Our contributions are as follows:

- We propose a novel method MC<sup>2</sup> for integrating various single-concept customized models to synthesize composition of different customized concepts, which does not require joint training, model merging or additional condition information.
- With minor adjustments, MC<sup>2</sup> can be extended to enhance the compositional generation ability of existing text-to-image diffusion models.
- Extensive qualitative and quantitative evaluations demonstrate that our proposed MC<sup>2</sup> significantly improves the performance of customized multi-concept generation and compositional text-to-image generation, even surpassing previous methods that require additional training.

## 2 Related Work

**Customized multi-concept generation.** Customized generation methods [13, 43, 49] aim to generate images of a specified concept given a few user-provided images of the concept. Custom Diffusion [25] first proposes to extend the task to a multi-concept scenario, where the compositions of multiple customized concepts are expected. Custom Diffusion finetunes a diffusion model given reference images of multiple concepts or merges single-concept customized diffusion models with constrained optimization. SVDiff [16] proposes the data augmentation strategy Cut-Mix-Unmix which splices two reference images together for finetuning the diffusion model. Some works [29, 38, 47] separately train customized models for each concept then merge the models to get one customized model with their proposed formulas. Cones [29] additionally requires finetuning for the merged customized model for better generation quality. Mix-of-Show [15] trains ED-LoRAs for each concept then merges them into one ED-LoRA via gradient fusion. Cones 2 [30] finetunes the text encoder for each concept, then derives a token embedding for it. Cones 2 only uses the embeddings for each concept at inference. Compositional Inversion [53] finetunes token embeddings for each concept then composes them via their proposed spatial inversion. Gen4Gen [51] proposes a data generation pipeline for training multi-concept customized models. Encoder-based customization methods FastComposer [50] and Subject-Diffusion [32] also support multi-concept customization, which are orthogonal to our work. VideoDreamer [8] and CustomVideo [48] consider multi-concept customization for text-to-video generation with diffusion models. DreamMatcher [34] enhances existing customization methods with semantic matching. Concurrent work [55] proposes to compose multiple LoRAs for image generation, but not particularly for multi-concept customization. Another line of work [2, 3, 22] focuses on extracting mul-

multiple concepts or attributes from a single image. Break-A-Scene [3] proposes a masked diffusion loss and a cross-attention loss to encourage the disentanglement between the concepts during training.

MC<sup>2</sup> supports combining multiple separately trained customized models of different architectures, *e.g.* Textual Inversion [13], LoRA [21] and DreamBooth [43], without additional training or layout information.

**Compositional generation.** Text-to-image diffusion models sometimes fail to generate all the subjects mentioned in the input text prompt, and the involved attributes may be bound to incorrect subjects. Previous works [1, 5, 7, 12, 23, 28, 33, 41, 52] aim to address the problem without additional training. [5, 28] adopt the architecture of parallel diffusion models. [12] strengthens the semantic information of some selected word of the prompt. [1, 7, 33, 41] optimize the noise map to encourage the co-occurrence of the mentioned concepts. [23] modulates the guidance direction of diffusion models during inference. Concurrent work RealCompo [52] enhances text-to-image diffusion models with layout-to-image diffusion models to promote compositionality of the generated images, which is orthogonal to our work.

**Sampling guidance for diffusion models.** Guidance methods interfere with the sampling process of the diffusion models to achieve various effects. Some works [10, 19, 20, 36] improve the sampling quality of diffusion models or make the generation results more consistent with the input condition. Others [4, 9, 11, 14, 24] enable additional condition input for pretrained text-to-image diffusion models, to control layout, style or other attributes of the generated images.

### 3 Method

#### 3.1 Problem Definition

In the realm of customized multi-concept generation, the goal is to create images encompassing multiple user-specified concepts. Specifically, we focus on a scenario where we have access solely to the trained single-concept customized models  $\{\mathcal{G}_1, \mathcal{G}_2, \dots, \mathcal{G}_n\}$  for each concept. In this context, the reference images for each concept are not available. Our goal is to propose some structure  $\mathcal{S}$ , which composes the single-concept customized models to enable the synthesis of an image  $x$  that incorporates the  $n$  concepts. Namely we aim to construct  $\mathcal{S}$ , such that:

$$x = \mathcal{S}(\mathcal{G}_1, \mathcal{G}_2, \dots, \mathcal{G}_n)(p), \quad (1)$$

where  $p$  is the input text prompt.

#### 3.2 Preliminaries

Recent text-to-image diffusion models are typically based on Denoising Diffusion Probabilistic Models (DDPMs). DDPMs model image generation as a denoising process where an individual denoising step is formulated as:

$$x_{t-1} = x_t - \epsilon_\theta(x_t, t) + \mathcal{N}(0, \sigma_t^2 I), \quad (2)$$



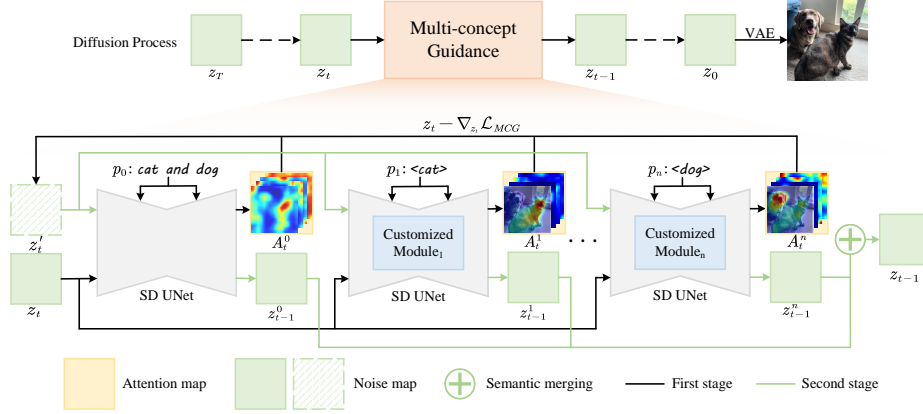


**Fig. 2: Illustration of our proposed MC<sup>2</sup>.** Multi-concept Guidance (MCG) is performed at each step of the diffusion process. In the first stage, several parallel diffusion models with different customized modules take the same noise map  $z_t$  as input.  $p_0$ ,  $p_1$  and  $p_n$  denote text prompts encoded by the CLIP text encoder. Then the cross-attention maps of certain tokens are extracted to compute the  $\mathcal{L}_{MCG}$  to update  $z_t$ . Figure 3 further visualizes the effect of  $\mathcal{L}_{MCG}$ . In the second stage, the diffusion models take  $z_t'$  as input and  $z_{t-1}$  is calculated via semantic merging. When omitting the customized modules and substituting  $\mathcal{L}_{CompGen}$  for  $\mathcal{L}_{MCG}$ , the framework applies to plain compositional generation.

where image  $x_{t-1}$  is a denoised version of  $x_t$ ,  $\epsilon_\theta$  is a model to predict the noise in  $x_t$ ,  $\mathcal{N}$  is a Gaussian distribution with learned covariance matrix  $\sigma_t^2 I$ . The denoising step is performed  $T$  times to get the final output image  $x_0$ .  $x_T$  is sampled from a Gaussian prior.  $\epsilon_\theta(x_t, t)$  is also called the score function of the diffusion model.

Composable Diffusion [28] shows that diffusion models are functionally similar to Energy Based Models (EBMs). Multiple EBMs can be composed to get a new EBM that models a composed distribution of the distributions modeled by the multiple EBMs. A trained diffusion model  $\epsilon_\theta(x_t, t)$  can be viewed as an implicitly parameterized EBM. Then multiple diffusion models can be composed to obtain a new diffusion model. Let model  $\mathcal{G}_i$  contain concept  $c_i$ , then an image containing  $c_i$  can be sampled using the score function  $\epsilon_\theta(x_t, t|c_i)$  of the conditional distribution  $p(x|c_i)$ . We then sample from the conditional distribution  $p(x|c_1, \dots, c_n)$  with the composed score function  $\hat{\epsilon}_\theta(x_t, t)$ :

$$\hat{\epsilon}_\theta(x_t, t) = \epsilon_\theta(x_t, t) + \sum_{i=1}^n w_i (\epsilon_\theta^i(x_t, t|c_i) - \epsilon_\theta(x_t, t)), \quad (3)$$

where  $w_i$  is a hyperparameter corresponding to the temperature scaling on concept  $c_i$ . For more detailed derivation, please refer to [28].

Equation (3) can act as the structure  $\mathcal{S}$  in Eq. (1), but it may confuse objects' attributes or create an object that merges the specified concepts, as shown in the

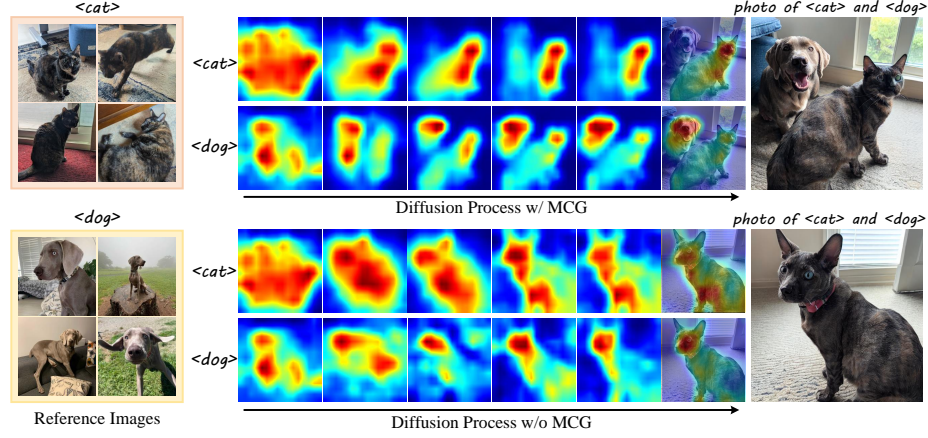


**Fig. 3: Visualization of MCG.** MCG adaptively refines the attention weights between visual and textual tokens, directing image regions to focus on their associated words while diminishing the impact of irrelevant ones. The reference images are from CustomConcept101 [25].

second row of Fig. 3 and the first row of Fig. 5. Composable LoRA [37] proposes to use the structure with LoRAs [44], *i.e.* to merge the concepts contained in different LoRA modules. As shown in Fig. 2, we adopt the architecture of multiple parallel diffusion models with different customized modules to start with. Limited by [28], the diffusion models are the instances of the same model. With this architecture, the customized modules can be of different forms, *e.g.* Textual Inversion [13], LoRA [21] and DreamBooth [43], as they are not required to be merged to one model, as shown in Fig. 1.

### 3.3 Multi-concept Guidance

Our proposed MC<sup>2</sup> performs Multi-concept Guidance (MCG) at each step of the diffusion process. At each step of the diffusion process we refine the attention weights between visual and textual tokens in order to spatially disentangle the customized concepts. We define a loss objective to measure the extent to which the customized concepts are spatially disentangled. As illustrated in Fig. 2, the noised latent map  $z_t$  is updated with the objective in the first stage. In the second stage, the diffusion models take the updated noised latent map  $z'_t$  as input and  $z_{t-1}$  is produced via semantic merging for the next denoising step.

We attempt to measure the extent to which the customized concepts are spatially disentangled with the help of the cross-attention maps generated at each step of the diffusion process. They can be regarded as features showing how strongly each latent image patch is associated with each text token embedding. Each cross-attention layer in the unet takes latent image features  $f \in \mathbb{R}^{(h \times w) \times l}$  and text features  $c \in \mathbb{R}^{s \times d}$  as input. After linear transformation  $Q = W^Q f$ ,

$K = W^K c$ ,  $V = W^V c$ , the attention maps are then:

$$A = \text{Softmax}\left(\frac{QK^T}{\sqrt{d'}}\right) \in \mathbb{R}^{(h \times w) \times s} \quad (4)$$

As Shown in Fig. 2, we first construct  $n + 1$  sub-prompts  $\{p_0, p_1, \dots, p_n\}$  for the diffusion models, where  $n$  denotes the number of customized concepts. Each concept is customized by a customized module.  $p_0$  describes the image to be generated as a whole.  $p_1$  to  $p_n$  describe each customized concept. The *trigger words* of the customized modules are included in their sub-prompts. Single-concept models typically have their trigger words for activating the customized information during the generation process. For Textual Inversion [13], the trigger word is the trained token embedding itself. For DreamBooth [43], the trigger words are some rare tokens selected from the vocabulary. We extract the cross-attention maps corresponding to the trigger words as they indicate whether and where the customized concepts are activated in the generation. Different cross-attention layers in the Stable Diffusion produce attention maps of different resolutions. Following [7], we empirically choose the  $16 \times 16$  attention maps. Then we average all the attention layers and heads to get the final attention map  $A \in \mathbb{R}^{h \times w}$ .

When a trigger word of a customized concept contains multiple tokens, each token may correspond to different part of the concept. Intuitively, we want the activated regions to stay close to each other, or to have more overlap. Inspired by [1], we encourage the IoU of the activated regions of the trigger tokens to be higher. Let  $A_i^k \in \mathbb{R}^{h \times w}$  represent the attention map corresponding to the  $i$ -th token within the  $k$ -th sub-prompt, while  $S_k$  signifies the collection of trigger token indices associated the  $k$ -th sub-prompt. Our proposed *intra-prompt aggregation loss* is defined as:

$$\mathcal{L}_{intra} = \frac{1}{n} \sum_{k=1}^n \frac{2}{(|S_k| - 1) |S_k|} \sum_{\substack{i, j \in S_k \\ \forall i < j}} \left(1 - \frac{\min(A_i^k, A_j^k)}{A_i^k + A_j^k}\right), \quad (5)$$

where the min operation is performed at the pixel dimension.

To spatially disentangle different customized concepts, we define another loss term to encourage less overlap of the regions activated by different customized modules. For sub-prompt  $p_k$ , we first aggregate the attention maps of the trigger tokens to get one attention map. Here, we empirically average the attention maps. After being smoothed by a Gaussian filter, we get the final attention map  $A^k \in \mathbb{R}^{h \times w}$  indicating the activated region of the customized concept. Figure 3 visualizes the attention maps of the involved concepts. Our proposed *inter-prompt disentanglement loss* is then:

$$\mathcal{L}_{inter} = \frac{2}{(n-1)n} \sum_{0 < i < j \leq n} \frac{\min(A^i, A^j)}{A^i + A^j}. \quad (6)$$

The overall loss objective is a linear combination of  $\mathcal{L}_{inter}$  and  $\mathcal{L}_{intra}$  with coefficient  $\alpha$ , and  $z_t$  is updated to  $z'_t$  with learning rate  $\lambda$ :

$$\mathcal{L}_{MCG} = \mathcal{L}_{inter} + \alpha \cdot \mathcal{L}_{intra}, \quad (7)$$

$$z'_t = z_t - \lambda \cdot \nabla_{z_t} \mathcal{L}_{MCG}. \quad (8)$$

Then the diffusion models take  $z'_t$  as input, and  $z_{t-1}$  is calculated via semantic merging:

$$z_{t-1} = z_{t-1}^u + \sum_{i=0}^n w_i (z_{t-1}^i - z_{t-1}^u). \quad (9)$$

The coefficients  $\{w_i\}_n$  controls the intensity of the customized concepts. Equation (9) can be seen as a implementation of Eq. (3), or be regarded as an extension of classifier-free guidance [19]. The unconditional output  $z_{t-1}^u$  is produced by the uncustomized diffusion model with blank text input, which is omitted in Fig. 2 for simplicity.

Our method can be extended to enhance the compositional capabilities of text-to-image generation. The customized modules are omitted as customization is not needed in such setting. Besides  $\mathcal{L}_{intra}$  and  $\mathcal{L}_{inter}$ , we also include  $\mathcal{L}_{A\&E}$  proposed by [7].  $\mathcal{L}_{A\&E}$  attempts to maximize the attention values for each subject token so as to encourage the occurrence of the subject. For a subject name that has multiple tokens, we empirically average the attention maps corresponding to each of them. Then the loss objective for compositional generation is defined as:

$$\mathcal{L}_{CompGen} = \mathcal{L}_{A\&E} + \alpha_1 \cdot \mathcal{L}_{intra} + \alpha_2 \cdot \mathcal{L}_{inter}, \quad (10)$$

$$\mathcal{L}_{A\&E} = \max_{A \in S_A} (1 - \max(A)), \quad (11)$$

where  $S_A$  is the set of attention maps corresponding to the subject names.

## 4 Experiments

### 4.1 Experiment Setup

**Datasets.** For customized multi-concept generation, we perform experiments on the CustomConcept101 dataset [25], consisting of 101 concepts and 101 unique compositions among the concepts. Each concept possesses 3 to 15 images. Each composition involves two concepts, accompanied by 12 prompts, *e.g.* `photo of the {0} and {1}`.

For compositional generation, we perform experiments on the benchmark proposed by [7]. It contains three types of text prompts: (i) a `<animal A>` and a `<animal B>`, (ii) a `<animal>` and a `<color><object>`, and (iii) a `<color A><object A>` and a `<color B><object B>`. The dataset includes 276 prompts in total.



**Fig. 4: Qualitative comparisons of customized multi-concept generation methods.** In the first row are concept reference images from the CustomConcept101 dataset. Each concept possesses 3 to 15 reference images. Our method demonstrates more consistency with the reference images compared to the competing methods. And the competing methods sometimes omit the specified concepts.



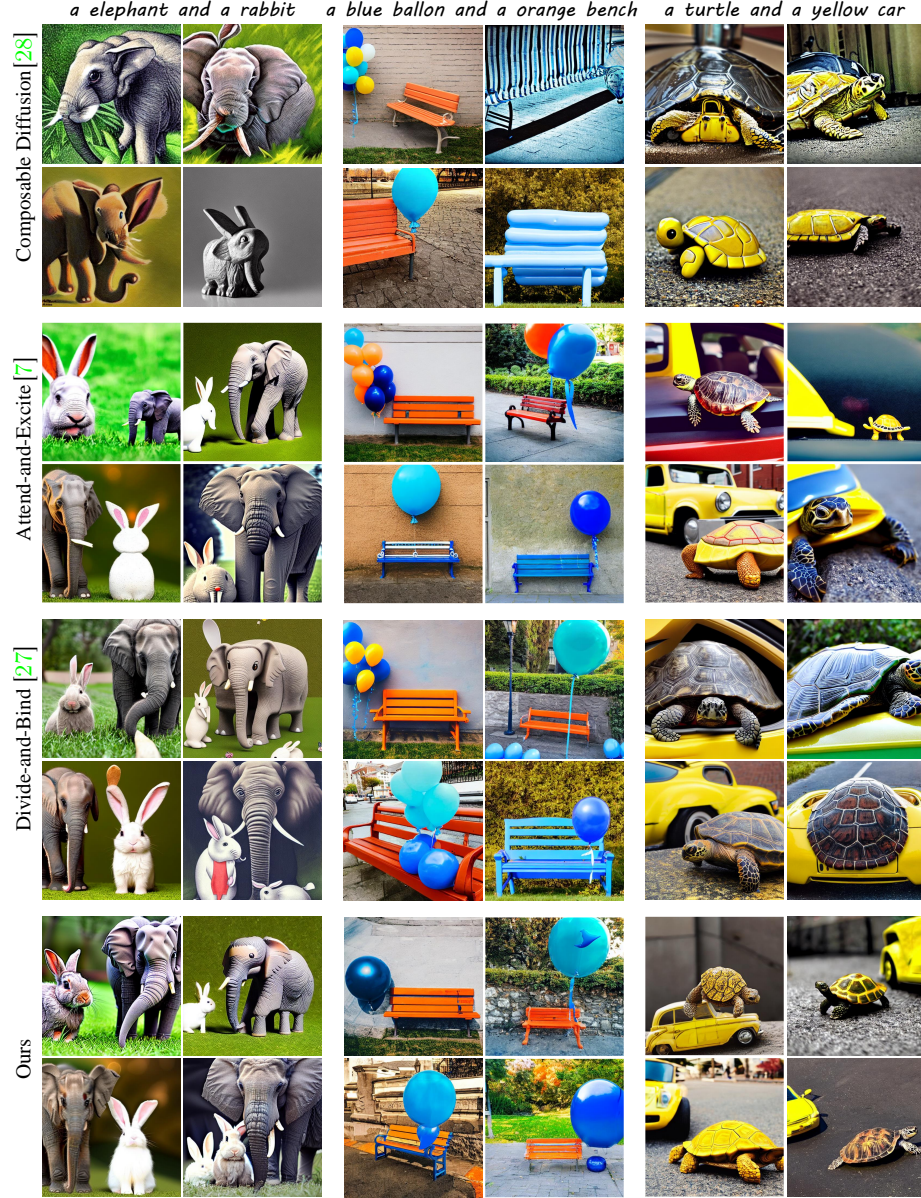


**Fig. 5: Qualitative comparisons of compositional generation techniques.** For each prompt, we show four images generated by each of the four considered methods where we use the same set of seeds across all approaches.

**Evaluation metrics.** For customized multi-concept generation, subject fidelity and prompt fidelity are evaluated, following [25, 43]. For subject fidelity, we compute two metrics: CLIP-I [13] and DINO [43]. CLIP-I is the average cosine similarity between CLIP [39] embeddings of generated and real images. The DINO metric is the average pairwise cosine similarity between the ViT-S/16 DINO [6] embeddings of generated and real images. For a composition of two concepts, CLIP-I and DINO metrics are computed for each concept respectively then averaged. Prompt fidelity is measured as the average cosine similarity between prompt and image CLIP embedding, denoted as CLIP-T [43]. The placeholder token in the text prompt template is replaced with the proper concept category for extracting CLIP text feature.

For compositional generation, we evaluate full prompt similarity, minimum object similarity and text-text similarity, following [7]. Full Prompt Similarity is similar to CLIP-T. To compute the Minimum Object Similarity, each prompt is split into two sub-prompts, each containing a single concept. We then compute the CLIP similarity between each sub-prompt and each generated image. Then the smaller of the two scores across all prompts are averaged to get the Minimum Object Similarity. To compute the text-text similarity, we employ BLIP [26] to generate captions for synthesized images, then measure the CLIP similarity between the original prompt and all captions.

**Baselines.** For customized multi-concept generation, we compare our method with Custom Diffusion [25], Mix-of-Show [15] and Cones 2 [30]. Custom Diffusion optimizes the cross-attention key and value parameter in the unet plus a token embedding given reference images. It either jointly train for multiple concepts or combine multiple finetuned models into one via closed-form constrained optimization, denoted as *Joint* and *Optimization* respectively. Mix-of-Show trains ED-LoRA for each concept, then fuses multiple ED-LoRAs into one via gradient fusion. ED-LoRA contains two token embeddings and LoRA [21] for the diffusion model. Mix-of-Show introduces regionally controllable sampling to control the location of each concept, which requires user-input bounding boxes for each concept, thus is omitted in our experiment. Cones 2 finetunes the text encoder for each concept. Then a residual token embedding is derived from the text encoder for inference. Cones 2 proposes a layout guidance which requires user-input location information. The layout guidance is omitted in our experiment. Textual Inversion [13] and DreamBooth [43] is not included here as they are not intended for customized multi-concept generation. Their performance can be found in [25].

For compositional generation, we compare our method with Attend-and-Excite [7], Divide-and-Bind [27] and Composable Diffusion [28]. Attend-and-Excite proposes a loss objective to maximize the attention values for each subject token. Divide-and-Bind proposes a attendance loss and a binding loss to better incorporate the semantics. For performance of Stable Diffusion v1-5 [42], please refer to [7].

**Implementation details.** We use the Stable Diffusion v1-5 in our experiments. Without loss of generality, we choose LoRA as the single-concept customized



**Table 1: Quantitative evaluation of customized multi-concept generation methods on CustomConcept101.** The metrics are first computed for each composition then averaged. CLIP-T measures prompt fidelity. CLIP-I and DINO measure subject fidelity.

Method	CLIP-T	CLIP-I	DINO
Custom Diffusion (Joint) [25]	0.789	0.645	0.339
Custom Diffusion (Optimization) [25]	0.788	0.646	0.339
Mix-of-Show [15]	0.728	0.670	0.394
Cones 2 [30]	<b>0.827</b>	0.624	0.264
Ours	0.767	<b>0.686</b>	<b>0.406</b>

**Table 2: Quantitative evaluation of compositional generation methods.** Metrics include *Full Prompt Similarity*, *Minimum Object Similarity* and *Text-Text Similarity*. The metrics are first computed for each prompt then averaged.

Method	Full Prompt	Min. Object	Text-Text
Composable Diffusion [28]	0.327	0.250	0.738
Attend-and-Excite [7]	0.352	0.264	0.818
Divide-and-Bind [27]	0.347	0.258	0.817
Ours	<b>0.356</b>	<b>0.266</b>	<b>0.833</b>

model, as different single-concept customization methods basically finetune some selected part of the diffusion model with similar loss functions. We adopt a popular community implementation of LoRA<sup>1</sup>. LoRA modules are trained for linear layers and  $1 \times 1$  conv layers in text encoder and unet with rank set to 16. We do not finetune the token embeddings. All reference images are captioned as `photo of a <concept name>`. Each concept has a unique `<concept name>` defined by CustomConcept101, *e.g.* `pet_dog1`. All LoRAs are trained for 1000 steps with batch size set to 2, learning rate set to  $1e-4$ . LoRA scale is set to 0.7 for merging the LoRA parameters into the diffusion model during inference. Unless mentioned otherwise, we use DPM++ sampler [31] with 30 sampling steps. Given a prompt template, *e.g.* `photo of the {0} and {1}`, we construct the sub-prompts for a composition as follows: (i) `photo of the <cate1> and <cate2>`, (ii) `photo of the <concept1> and <cate2>`, a `<concept1>`, (iii) `photo of the <cate1> and <concept2>`, a `<concept2>`. `<cate1>` is the category name of `<concept1>` defined by CustomConcept101, *e.g.* `dog` for `pet_dog1`.

## 4.2 Customized Multi-concept Generation Results

**Qualitative evaluation.** Figure 4 shows the generated images of our method and the baselines. Note that the problem definitions of [15, 25] slightly differ from the definition in Sec. 3.1, as they either require jointly training the two

<sup>1</sup> <https://github.com/kohya-ss/sd-scripts>

**Table 3: User study.** Twenty-eight users take part in the survey. The users are asked to select the image most consistent with the prompt (Text Alignment) and the reference images (Image Alignment).

Method	Text Align.	Image Align.	Method	Text Align.
Custom Diffusion	3.66%	7.77%	Composable Diffusion	1.19%
Mix-of-Show	8.66%	16.51%	Attend-and-Excite	10.00%
Cones 2	8.93%	2.32%	Divide-and-Bind	6.55%
Ours	<b>78.75%</b>	<b>73.39%</b>	Ours	<b>82.26%</b>

concepts or require training to merge the single-concept customized models. In our setting, the single-concept models are separately trained and directly used in inference. The baselines sometimes omit one of the specified concepts, *e.g.* the white chair for `<sofa>` and `<chair>` and the person for `<person>` and `<cat>`. Our method demonstrates higher fidelity to the reference images even compared to Custom Diffusion [25] that requires jointly training the two concepts, or Mix-of-Show [15] that requires training to merge the two single-concept customized models. Cones 2 [30] shows relatively low fidelity to the reference images, considering that it requires the least trained parameters.

**Quantitative evaluation.** We generate 16 samples per prompt with the same set of random seeds, resulting in a total of 19392 images for each method. As shown in Tab. 1, our method outperforms the baselines in terms of subject fidelity. Though [30] achieves a relatively higher CLIP-T score, it shows rather low subject fidelity. As mentioned in Sec. 4.1, CLIP-T is the similarity between the customized images and uncustomized text prompt. The prompt `cat` may be more close to some random cat image rather than a customized cat photo. A relatively high CLIP-T score indicates that our method has higher subject fidelity while consistent with the input text prompt.

### 4.3 Compositional Generation Results

**Qualitative evaluation.** Figure 5 shows the generated images of our method and the baselines. Composable Diffusion [28] sometimes merges the two objects, *e.g.* the bench made of blue balloon. Attend-and-Excite [7] and Divide-and-Bind [27] come across incorrect attribute binding problem, *e.g.* the rabbit with ivories, the blue bench. While our method successfully generates the objects without confusing the attributes belonging to each object.

**Quantitative evaluation.** We generate 16 samples per prompt with the same set of random seeds, resulting in a total of 4416 images for each method. As shown in Tab. 2, our method outperforms the baselines.

### 4.4 User Study

We perform a user study to evaluate our method. For customized multi-concept generation, we show users the generated images of each method along with two

**Table 4: Ablation Study.** The underline shows the second highest scores. No prefix appended to the sub-prompts leads to lower prompt fidelity, although subject fidelity slightly increases. No  $\mathcal{L}_{intra}$  increases prompt fidelity slightly, but subject fidelity drops.

Method	Customization			Compositional Gen.		
	CLIP-T	CLIP-I	DINO	Full.	Min.	T-T
Ours	<u>0.771</u>	<u>0.714</u>	<u>0.433</u>	<b>0.356</b>	<b>0.266</b>	<b>0.833</b>
Ours w/o first model	0.764	0.711	0.425	0.349	0.263	0.809
Ours w/o prefix	0.632	<b>0.736</b>	<b>0.476</b>	0.354	0.266	0.822
Ours w/o $\mathcal{L}_{intra}$	<b>0.773</b>	0.710	0.432	0.355	0.264	0.830
Ours w/o $\mathcal{L}_{intra}, \mathcal{L}_{inter}$	0.769	0.706	0.417	0.353	0.263	0.827

reference images of the concept. Then the users are asked to select the image that is most consistent with the prompt and the image that best represents the concepts. For compositional generation, we show users the generated images of each method and ask them to choose the one most consistent with the prompt. The questionnaire contains 40 questions for the customization task and 30 questions for compositional generation. We collect 28 responses in total. As shown in Tab. 3, our method outperforms the baselines.

#### 4.5 Ablation Study

To save computational expense, the ablation for customized multi-concept generation is carried out on a subset of CustomConcept101, which contains ten randomly selected compositions. Each composition is accompanied by 12 prompts. For compositional generation, we use the full benchmark dataset mentioned in Sec. 4.1.

**The loss objectives.** Without the two proposed loss terms, subject fidelity and prompt fidelity drop. Though  $\mathcal{L}_{intra}$  harms prompt fidelity slightly, we include it to achieve a overall better result. As shown in Fig. 6, the fidelity to the reference images decreases when omitting the loss terms.

**Architecture.** As shown in Fig. 2, the first diffusion model is not equipped with any customized modules and is conditioned on prompt  $p_0$  which describes the whole scene. We omit the first diffusion model then all the metrics decrease, as in the second row of Tab. 4. As shown in the third column of Fig. 6, mountains in the background are not generated without the first model.

**Construction of sub-prompts.** As mentioned in implementation details in Sec. 4.1, we append  $p_0$  to  $p_1, \dots, p_n$  as prefix to improve the consistency with the original input prompt, inspired by [17]. Without the prefix appended, the prompt fidelity drops, indicating the effect of this component to increase the consistency with the input prompt. The subject fidelity increases slightly as the model has more freedom to depict the concepts but with less control from the original prompt. In the fourth column of Fig. 6, mountains and city are not generated without the prefix.

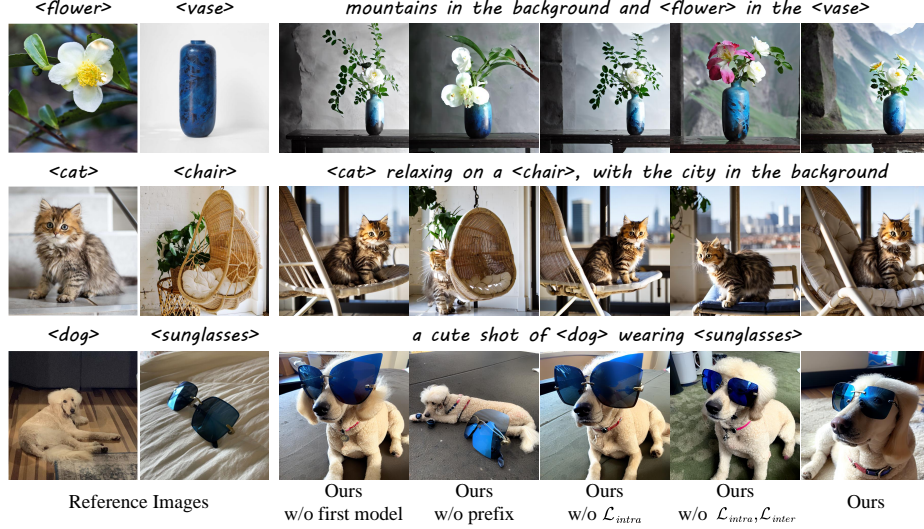


**Fig. 6: Qualitative comparisons of ablation variants.** Omitting any of the components harms the generation quality, resulting in lower fidelity to the text prompts and reference images.

## 5 Conclusion

In conclusion, we have proposed MC<sup>2</sup> which allows combination of various heterogeneous single-concept customized models, enabling a more flexible customized multi-concept generation with improved fidelity. Multiple customized models are seamlessly integrated with Multi-concept Guidance to synthesize a natural composition of the multiple customized concepts, without additional training. MC<sup>2</sup> can further be extended to elevate the compositional capabilities of text-to-image generation.

## References

1. Agarwal, A., Karanam, S., Joseph, K.J., Saxena, A., Goswami, K., Srinivasan, B.V.: A-STAR: test-time attention segregation and retention for text-to-image synthesis. In: IEEE/CVF International Conference on Computer Vision, ICCV 2023, Paris, France, October 1-6, 2023. pp. 2283–2293. IEEE (2023)
2. Agarwal, A., Karanam, S., Shukla, T., Srinivasan, B.V.: An image is worth multiple words: Multi-attribute inversion for constrained text-to-image synthesis. arXiv preprint arXiv:2311.11919 (2023)
3. Avrahami, O., Aberman, K., Fried, O., Cohen-Or, D., Lischinski, D.: Break-a-scene: Extracting multiple concepts from a single image. In: SIGGRAPH Asia 2023 Conference Papers. pp. 1–12 (2023)
4. Bansal, A., Chu, H.M., Schwarzschild, A., Sengupta, S., Goldblum, M., Geiping, J., Goldstein, T.: Universal guidance for diffusion models. In: Proceedings of the

- IEEE/CVF Conference on Computer Vision and Pattern Recognition. pp. 843–852 (2023)
5. Bar-Tal, O., Yariv, L., Lipman, Y., Dekel, T.: Multidiffusion: Fusing diffusion paths for controlled image generation. In: International Conference on Machine Learning (2023)
  6. Caron, M., Touvron, H., Misra, I., Jégou, H., Mairal, J., Bojanowski, P., Joulin, A.: Emerging properties in self-supervised vision transformers. In: Proceedings of the IEEE/CVF international conference on computer vision. pp. 9650–9660 (2021)
  7. Chefer, H., Alaluf, Y., Vinker, Y., Wolf, L., Cohen-Or, D.: Attend-and-excite: Attention-based semantic guidance for text-to-image diffusion models. *ACM Transactions on Graphics (TOG)* **42**, 1 – 10 (2023)
  8. Chen, H., Wang, X., Zeng, G., Zhang, Y., Zhou, Y., Han, F., Zhu, W.: Videodreamer: Customized multi-subject text-to-video generation with disen-mix fine-tuning. *arXiv preprint arXiv:2311.00990* (2023)
  9. Chen, M., Laina, I., Vedaldi, A.: Training-free layout control with cross-attention guidance. In: Proceedings of the IEEE/CVF Winter Conference on Applications of Computer Vision. pp. 5343–5353 (2024)
  10. Dhariwal, P., Nichol, A.: Diffusion models beat gans on image synthesis. *Advances in neural information processing systems* **34**, 8780–8794 (2021)
  11. Epstein, D., Jabri, A., Poole, B., Efros, A., Holynski, A.: Diffusion self-guidance for controllable image generation. *Advances in Neural Information Processing Systems* **36** (2024)
  12. Feng, W., He, X., Fu, T.J., Jampani, V., Akula, A.R., Narayana, P., Basu, S., Wang, X.E., Wang, W.Y.: Training-free structured diffusion guidance for compositional text-to-image synthesis. In: The Eleventh International Conference on Learning Representations (2022)
  13. Gal, R., Alaluf, Y., Atzmon, Y., Patashnik, O., Bermano, A.H., Chechik, G., Cohen-or, D.: An image is worth one word: Personalizing text-to-image generation using textual inversion. In: The Eleventh International Conference on Learning Representations (2022)
  14. Ge, S., Park, T., Zhu, J.Y., Huang, J.B.: Expressive text-to-image generation with rich text. In: Proceedings of the IEEE/CVF International Conference on Computer Vision. pp. 7545–7556 (2023)
  15. Gu, Y., Wang, X., Wu, J.Z., Shi, Y., Yunpeng, C., Fan, Z., Xiao, W., Zhao, R., Chang, S., Wu, W., Ge, Y., Ying, S., Shou, M.Z.: Mix-of-show: Decentralized low-rank adaptation for multi-concept customization of diffusion models. *arXiv preprint arXiv:2305.18292* (2023)
  16. Han, L., Li, Y., Zhang, H., Milanfar, P., Metaxas, D.N., Yang, F.: Svdiff: Compact parameter space for diffusion fine-tuning. In: IEEE/CVF International Conference on Computer Vision, ICCV 2023, Paris, France, October 1-6, 2023. pp. 7289–7300. IEEE (2023)
  17. Hertz, A., Mokady, R., Tenenbaum, J., Aberman, K., Pritch, Y., Cohen-or, D.: Prompt-to-prompt image editing with cross-attention control. In: The Eleventh International Conference on Learning Representations (2022)
  18. Ho, J., Jain, A., Abbeel, P.: Denoising diffusion probabilistic models. *Advances in neural information processing systems* **33**, 6840–6851 (2020)
  19. Ho, J., Salimans, T.: Classifier-free diffusion guidance. In: NeurIPS 2021 Workshop on Deep Generative Models and Downstream Applications (2021)
  20. Hong, S., Lee, G., Jang, W., Kim, S.: Improving sample quality of diffusion models using self-attention guidance. In: Proceedings of the IEEE/CVF International Conference on Computer Vision. pp. 7462–7471 (2023)

21. Hu, E.J., Shen, Y., Wallis, P., Allen-Zhu, Z., Li, Y., Wang, S., Wang, L., Chen, W.: LoRA: Low-rank adaptation of large language models. In: International Conference on Learning Representations (2022)
22. Jin, C., Tanno, R., Saseendran, A., Diethe, T., Teare, P.: An image is worth multiple words: Learning object level concepts using multi-concept prompt learning. arXiv preprint arXiv:2310.12274 (2023)
23. Kang, H., Lee, D., Shin, M., Lee, I.K.: Semantic guidance tuning for text-to-image diffusion models. arXiv preprint arXiv:2312.15964 (2023)
24. Kim, Y., Lee, J., Kim, J.H., Ha, J.W., Zhu, J.Y.: Dense text-to-image generation with attention modulation. In: Proceedings of the IEEE/CVF International Conference on Computer Vision. pp. 7701–7711 (2023)
25. Kumari, N., Zhang, B., Zhang, R., Shechtman, E., Zhu, J.Y.: Multi-concept customization of text-to-image diffusion. In: Proceedings of the IEEE/CVF Conference on Computer Vision and Pattern Recognition. pp. 1931–1941 (2023)
26. Li, J., Li, D., Xiong, C., Hoi, S.: Blip: Bootstrapping language-image pre-training for unified vision-language understanding and generation. In: International Conference on Machine Learning. pp. 12888–12900. PMLR (2022)
27. Li, Y., Keuper, M., Zhang, D., Khoreva, A.: Divide & bind your attention for improved generative semantic nursing. In: 34th British Machine Vision Conference 2023. p. 366. BMVA Press (2023)
28. Liu, N., Li, S., Du, Y., Torralba, A., Tenenbaum, J.B.: Compositional visual generation with composable diffusion models. In: European Conference on Computer Vision. pp. 423–439. Springer (2022)
29. Liu, Z., Feng, R., Zhu, K., Zhang, Y., Zheng, K., Liu, Y., Zhao, D., Zhou, J., Cao, Y.: Cones: Concept neurons in diffusion models for customized generation. In: Krause, A., Brunskill, E., Cho, K., Engelhardt, B., Sabato, S., Scarlett, J. (eds.) International Conference on Machine Learning, ICML 2023, 23–29 July 2023, Honolulu, Hawaii, USA. Proceedings of Machine Learning Research, vol. 202, pp. 21548–21566. PMLR (2023)
30. Liu, Z., Zhang, Y., Shen, Y., Zheng, K., Zhu, K., Feng, R., Liu, Y., Zhao, D., Zhou, J., Cao, Y.: Cones 2: Customizable image synthesis with multiple subjects. arXiv preprint arXiv:2305.19327 (2023)
31. Lu, C., Zhou, Y., Bao, F., Chen, J., Li, C., Zhu, J.: Dpm-solver++: Fast solver for guided sampling of diffusion probabilistic models. arXiv preprint arXiv:2211.01095 (2022)
32. Ma, J., Liang, J., Chen, C., Lu, H.: Subject-diffusion: Open domain personalized text-to-image generation without test-time fine-tuning. arXiv preprint arXiv:2307.11410 (2023)
33. Meral, T.H.S., Simsar, E., Tombari, F., Yanardag, P.: Conform: Contrast is all you need for high-fidelity text-to-image diffusion models. arXiv preprint arXiv:2312.06059 (2023)
34. Nam, J., Kim, H., Lee, D., Jin, S., Kim, S., Chang, S.: Dreammatcher: Appearance matching self-attention for semantically-consistent text-to-image personalization. arXiv preprint arXiv:2402.09812 (2024)
35. Ni, M., Zhang, Y., Feng, K., Li, X., Guo, Y., Zuo, W.: Ref-diff: Zero-shot referring image segmentation with generative models. arXiv preprint arXiv:2308.16777 (2023)
36. Nichol, A., Dhariwal, P., Ramesh, A., Shyam, P., Mishkin, P., McGrew, B., Sutskever, I., Chen, M.: Glide: Towards photorealistic image generation and editing with text-guided diffusion models. In: International Conference on Machine Learning (2021)

37. Opparco: Composable lora (2023), <https://github.com/opparco/stable-diffusion-webui-composable-lora>
38. Po, R., Yang, G., Aberman, K., Wetzstein, G.: Orthogonal adaptation for modular customization of diffusion models. arXiv preprint arXiv:2312.02432 (2023)
39. Radford, A., Kim, J.W., Hallacy, C., Ramesh, A., Goh, G., Agarwal, S., Sastry, G., Askell, A., Mishkin, P., Clark, J., et al.: Learning transferable visual models from natural language supervision. In: International conference on machine learning. pp. 8748–8763. PMLR (2021)
40. Ramesh, A., Dhariwal, P., Nichol, A., Chu, C., Chen, M.: Hierarchical text-conditional image generation with clip latents. arXiv preprint arXiv:2204.06125 (2022)
41. Rassin, R., Hirsch, E., Glickman, D., Ravfogel, S., Goldberg, Y., Chechik, G.: Linguistic binding in diffusion models: Enhancing attribute correspondence through attention map alignment. arXiv preprint arXiv:2306.08877 (2023)
42. Rombach, R., Blattmann, A., Lorenz, D., Esser, P., Ommer, B.: High-resolution image synthesis with latent diffusion models. 2022 IEEE/CVF Conference on Computer Vision and Pattern Recognition (CVPR) pp. 10674–10685 (2021)
43. Ruiz, N., Li, Y., Jampani, V., Pritch, Y., Rubinstein, M., Aberman, K.: Dreambooth: Fine tuning text-to-image diffusion models for subject-driven generation. In: Proceedings of the IEEE/CVF Conference on Computer Vision and Pattern Recognition. pp. 22500–22510 (2023)
44. Ryu, S.: Low-rank adaptation for fast text-to-image diffusion fine-tuning (2022), <https://github.com/cloneofsimon/lora>
45. Saharia, C., Chan, W., Saxena, S., Li, L., Whang, J., Denton, E.L., Ghasemipour, K., Gontijo Lopes, R., Karagol Ayan, B., Salimans, T., et al.: Photorealistic text-to-image diffusion models with deep language understanding. Advances in Neural Information Processing Systems **35**, 36479–36494 (2022)
46. Tang, R., Liu, L., Pandey, A., Jiang, Z., Yang, G., Kumar, K., Stenetorp, P., Lin, J., Ture, F.: What the DAAM: interpreting stable diffusion using cross attention. In: ACL (1). pp. 5644–5659. Association for Computational Linguistics (2023)
47. Tewel, Y., Gal, R., Chechik, G., Atzmon, Y.: Key-locked rank one editing for text-to-image personalization. In: ACM SIGGRAPH 2023 Conference Proceedings. pp. 1–11 (2023)
48. Wang, Z., Li, A., Xie, E., Zhu, L., Guo, Y., Dou, Q., Li, Z.: Customvideo: Customizing text-to-video generation with multiple subjects. arXiv preprint arXiv:2401.09962 (2024)
49. Wei, Y., Zhang, Y., Ji, Z., Bai, J., Zhang, L., Zuo, W.: Elite: Encoding visual concepts into textual embeddings for customized text-to-image generation. arXiv preprint arXiv:2302.13848 (2023)
50. Xiao, G., Yin, T., Freeman, W.T., Durand, F., Han, S.: Fastcomposer: Tuning-free multi-subject image generation with localized attention. arXiv preprint arXiv:2305.10431 (2023)
51. Yeh, C.H., Cheng, T.Y., Hsieh, H.Y., Lin, C.E., Ma, Y., Markham, A., Trigoni, N., Kung, H., Chen, Y.: Gen4gen: Generative data pipeline for generative multi-concept composition. arXiv preprint arXiv:2402.15504 (2024)
52. Zhang, X., Yang, L., Cai, Y., Yu, Z., Xie, J., Tian, Y., Xu, M., Tang, Y., Yang, Y., Cui, B.: Realcompo: Dynamic equilibrium between realism and compositionality improves text-to-image diffusion models. arXiv preprint arXiv:2402.12908 (2024)
53. Zhang, X., Wei, X.Y., Wu, J., Zhang, T., Zhang, Z., Lei, Z., Li, Q.: Compositional inversion for stable diffusion models. In: Proceedings of the AAAI Conference on Artificial Intelligence. vol. 38, pp. 7350–7358 (2024)



- 54. Zhang, Y., Wei, Y., Jiang, D., Zhang, X., Zuo, W., Tian, Q.: Controlvideo: Training-free controllable text-to-video generation. arXiv preprint arXiv:2305.13077 (2023)
- 55. Zhong, M., Shen, Y., Wang, S., Lu, Y., Jiao, Y., Ouyang, S., Yu, D., Han, J., Chen, W.: Multi-lora composition for image generation. arXiv preprint arXiv:2402.16843 (2024)

## Appendix

In Appendix A, we show additional experimental results. In Appendix B, we show more implementation details. In Appendix C, Appendix D and Appendix E, we discuss the possible limitations, future work and societal impact of our work.

### A Additional Results

Figure 7 shows more qualitative comparisons of the proposed method and the baselines [15, 25, 30] on customized multi-concept generation. The prompts may contain other subjects besides the customized concepts, *e.g.* mountains and sunglasses. The fourth row shows the results on the composition of two concepts with similar appearance. The last three rows show results on editing the attribute of the customized concept, unreal composition of the concepts, and editing the style, respectively. Our method demonstrates a more satisfying effect.

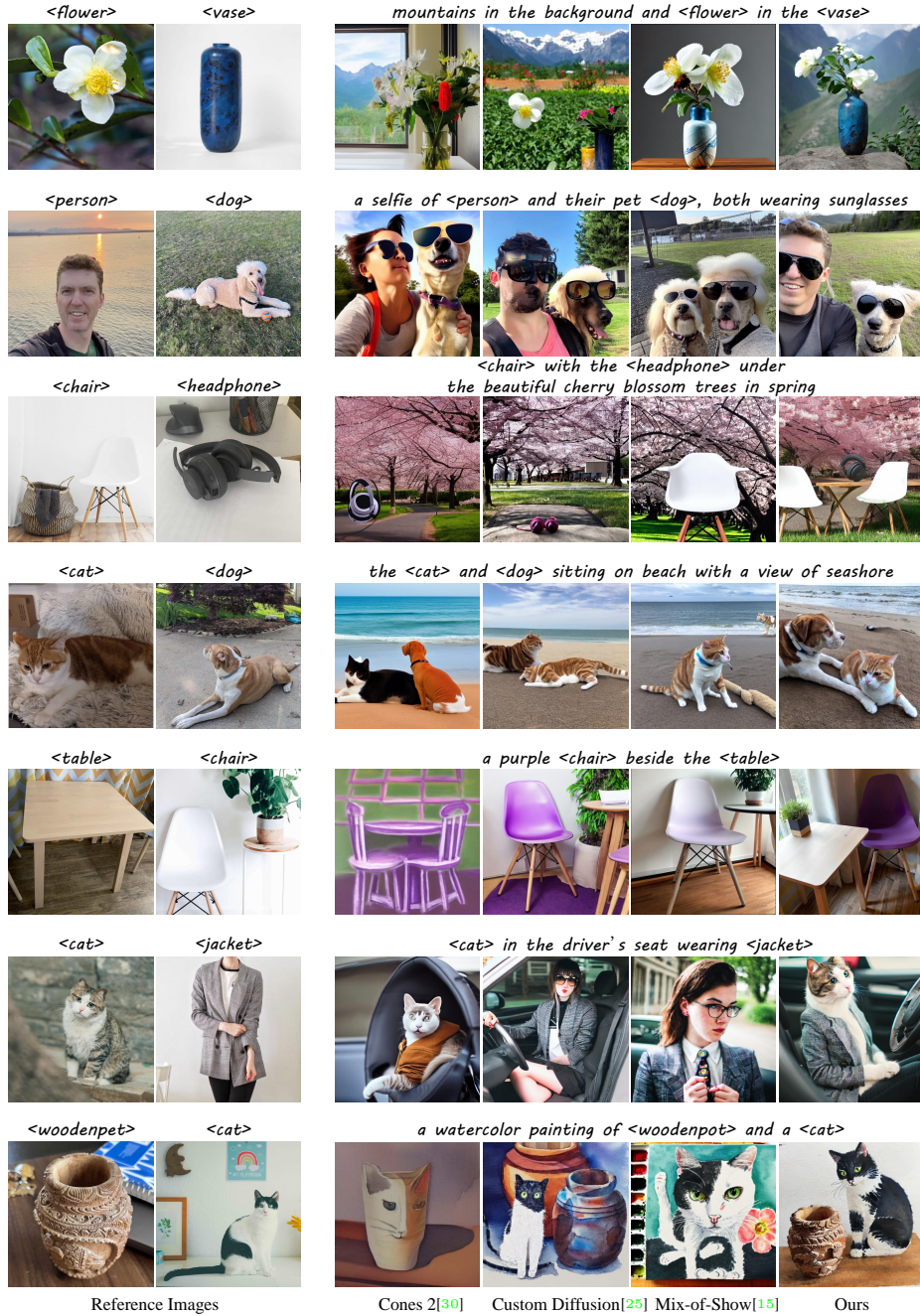
Figure 8 shows qualitative comparisons of the customized multi-concept generation methods on composition of three concepts. Our method demonstrates more higher fidelity to the reference images.

Figure 9 shows more qualitative comparisons of the compositional generation methods. Our method demonstrates better consistency with the input text prompts compared to the baselines [7, 27, 28].

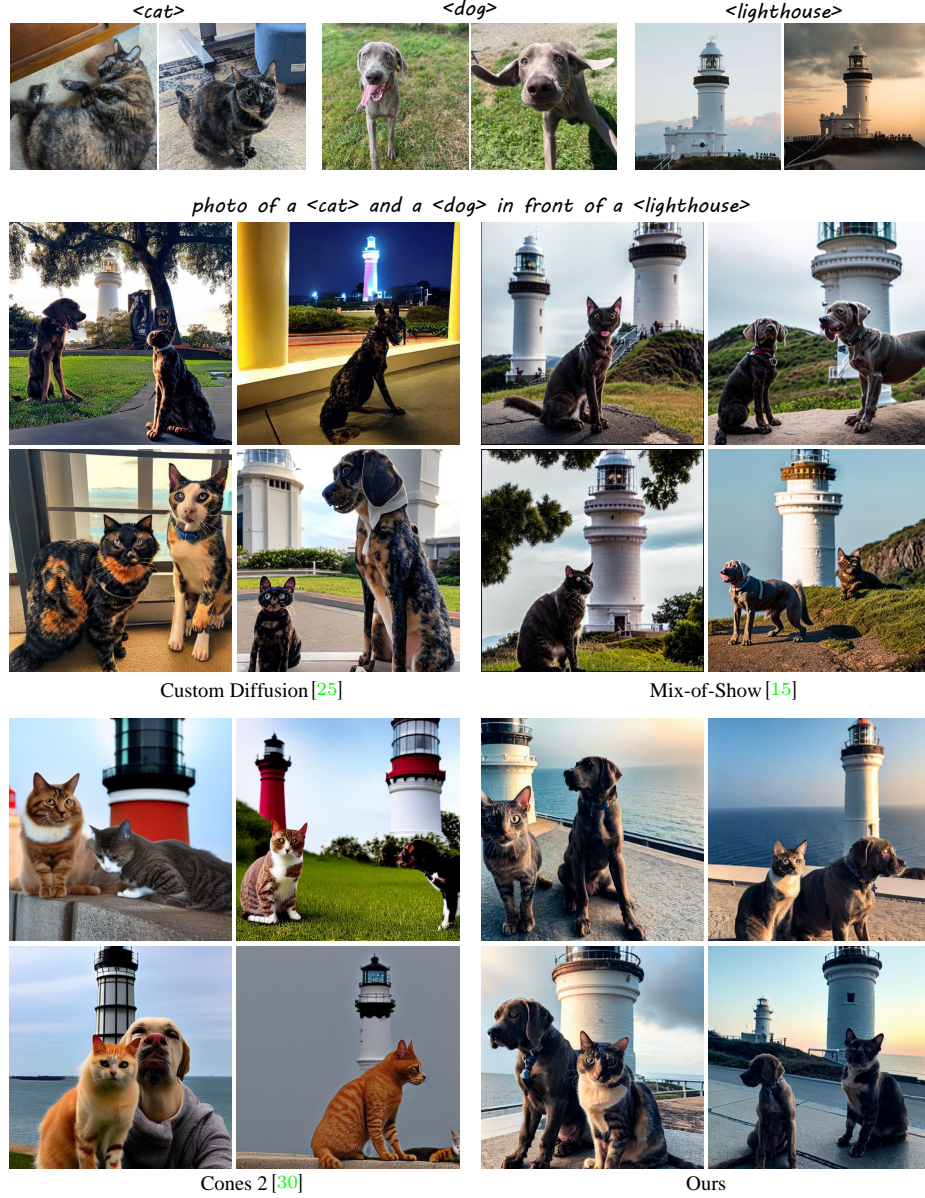
### B Implementation Details

Table 5 shows the computational demands associated with each customized multi-concept generation method. Our measurements are conducted on a desktop equipped with i5-13600K and RTX 3090. The first column shows the storage requirement for a single concept. The comparatively lower storage demand of Mix-of-Show is partly due to its DropLoRA training strategy. This approach encourages the token embedding rather than the LoRA module to learn more of the concept, thus limiting its performance. We train all the models with `fp16` mixed precision for 1000 steps, employing a batch size set of 2. The second column shows the training time of Custom Diffusion (Joint) on a composition of two concepts, and training time of other methods for a single concept. Custom Diffusion (Optimization) and Mix-of-Show require additional time for merging the single-concept models. Our method requires relatively longer inference time as it performs inference time optimization.

The coefficients  $\alpha, \alpha_1, \alpha_2$  are set to 0.8, 0.5, 0.4, respectively. For customized multi-concept generation,  $w_0, w_1, w_2$  are set to 1.4, 5.6, 5.6, respectively. For compositional generation,  $w_0, w_1, w_2$  are set to 5.6, 1.4, 1.4, respectively. The MCG is performed at the first 25 steps of the diffusion process. The Gaussian filter used to smooth the cross-attention maps has a kernel size of 3 and a standard deviation of 0.5.



**Fig. 7: Qualitative comparisons of customized multi-concept generation methods.** The reference images and text prompts are from the CustomConcept101 dataset [25].



**Fig. 8: Qualitative comparisons of customized multi-concept generation methods.** The composition involves three customized concepts. The reference images and are from the CustomConcept101 dataset [25].



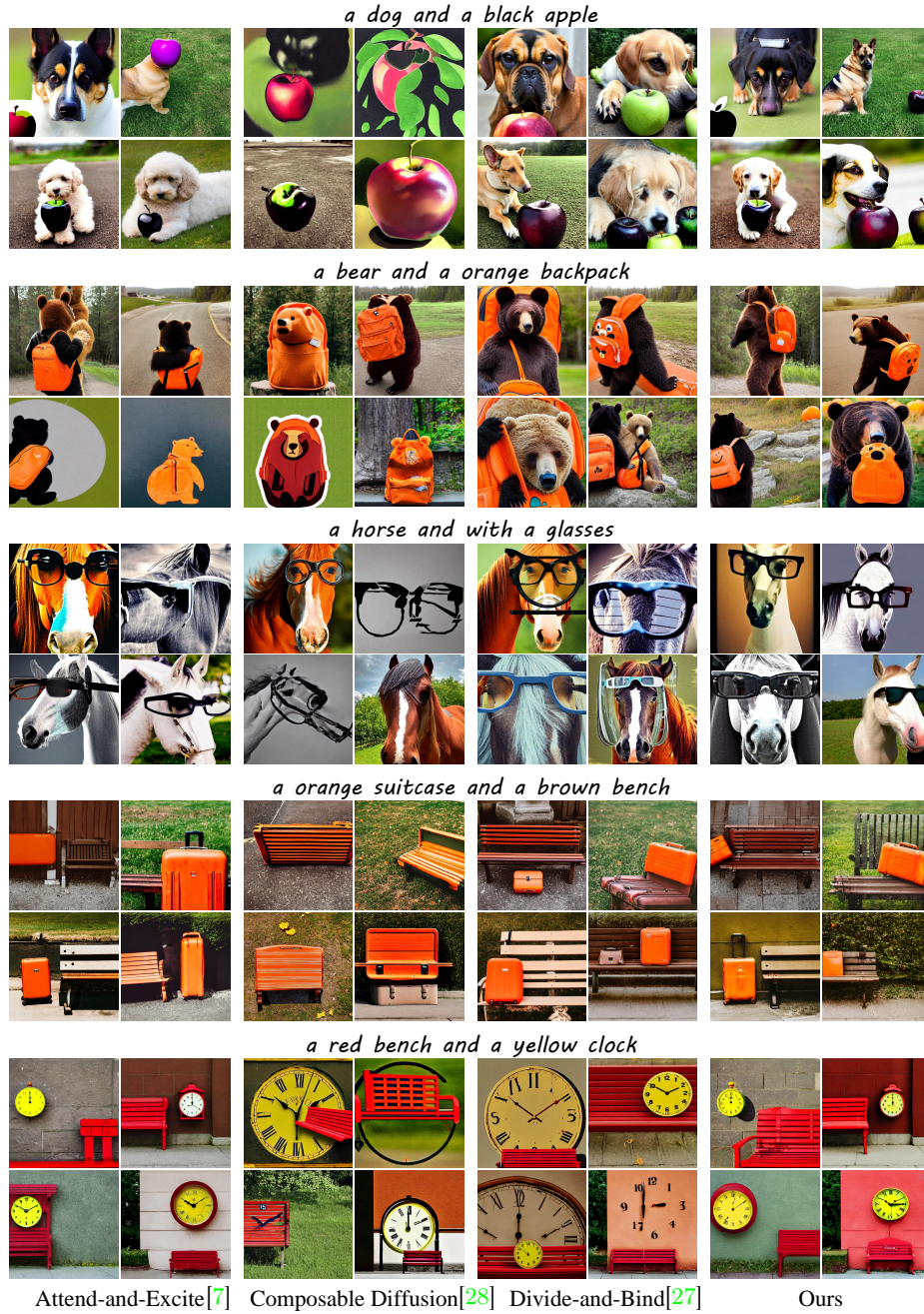


**Fig.9: Qualitative comparisons of compositional generation methods.** For each prompt, we show four images generated by each of the four considered methods where we use the same set of seeds across all approaches. The prompts are from the dataset introduced by [7].

**Table 5: Computational requirements of the customized multi-concept generation methods.** Here we list time and memory usage of each method.

Method	Storage	Training Time	Additional Time	Memory Usage	Inference Time
Custom Diff. (Joint) [25]	75MB	9min	–	4GB	2s
Custom Diff. (Optim.) [25]	75MB	5min	1min	4GB	2s
Mix-of-Show [15]	5MB	8min	3min	4GB	2s
Cones 2 [30]	5KB	8min	–	4GB	2s
Ours	38MB	7min	–	10GB	8s

## C Limitations

A limitation of our method is that the architecture of multiple parallel diffusion models requires relatively larger memory usage, particularly when composing multiple customized concepts. This is partly due to our implementation. We literally maintain multiple instances of the same diffusion model in memory for the sake of simplicity. Addressing this limitation involves optimizing memory utilization by storing only a single instance of the diffusion model in memory, thereby enhancing memory efficiency.

Despite MC<sup>2</sup> enables users to compose multiple separately trained, even heterogeneous customized models, the customized models should be trained from the same diffusion model. Such limitation is inherited from [28].

## D Future Work

In addition to addressing the limitations mentioned in Appendix C, there exist several promising avenues for future research. [8, 48] delve into the realm of multi-concept customization for text-to-video generation. An intriguing prospect is to investigate the adaptability of our proposed MC<sup>2</sup> to the domain of text-to-video generation. The existing benchmark dataset, CustomConcept101 [25], is currently limited to compositions of two concepts. To better evaluate the performance of methods in handling the composition of three or more concepts, it may prove beneficial to either develop a new dataset or expand upon the existing CustomConcept101.

For compositional generation, an interesting avenue for exploration involves building upon our methodology. Our approach not only addresses current challenges but also opens up a novel design space for further investigation. This provides a foundation for the development of innovative methods to enhance compositional generation techniques.

## E Societal Impact

First and foremost, MC<sup>2</sup> empowers users to effortlessly generate visually captivating compositions reflecting their unique ideas and preference. Additionally, MC<sup>2</sup>’s ability to enhance the capabilities of existing text-to-image diffusion models opens up new avenues for artistic exploration and innovation, potentially inspiring broader adoption and engagement in creative endeavors. However, MC<sup>2</sup>

may blur the lines between ethical and unethical image manipulation. Without proper guidance and ethical considerations, individuals may engage in harmful practices such as image forgery or digital impersonation. We advocate for the development of legal frameworks that address AI-generated content, including penalties for malicious use.